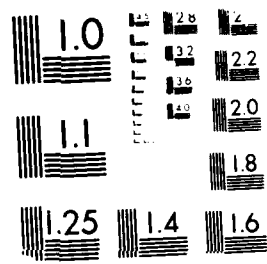


AD-A190 101 BASIC INSTABILITY MECHANISMS IN CHEMICALLY REACTING
SUBSONIC AND SUPERSONIC FLOWS (U) MASSACHUSETTS INST OF
TECH CAMBRIDGE 1100NG 23 OCT 87 AFOSR-IR-87-1689 1/1
UNCLASSIFIED AFOSR-83-0373 F/G 21/2 NL





MICROCOPY RESOLUTION TEST CHART
Nikon Corporation

Unclassified
SECURITY CLASSIFICATION OF THIS PAGE

AD-A190 101 (2)

Form Approved
OMB No. 0704-0188

REPORT DOCUMENT			
1a. REPORT SECURITY CLASSIFICATION Unclassified	DTIC	1b. RESTRICTIVE MARKINGS None	DTIC FILE COPY
2a. SECURITY CLASSIFICATION AUTHORITY ELECTED	S	3. DISTRIBUTION/AVAILABILITY OF REPORT Approved for public release; distribution is unlimited.	D
2b. DECLASSIFICATION/DOWNGRADING SCHEDULE JAN 14 1988	H	5. MONITORING ORGANIZATION REPORT NUMBER(S) AFOSR-TR-87-1889	D
4. PERFORMING ORGANIZATION REPORT NUMBER(S)			
6a. NAME OF PERFORMING ORGANIZATION Massachusetts Inst. of Tech.	6b. OFFICE SYMBOL (if applicable)	7a. NAME OF MONITORING ORGANIZATION AFOSR/NA	
6c. ADDRESS (City, State, and ZIP Code) Cambridge, MA 02139		7b. ADDRESS (City, State, and ZIP Code) Building 410, Bolling AFB DC 20332-6448	
8a. NAME OF FUNDING/SPONSORING ORGANIZATION AFOSR/NA	8b. OFFICE SYMBOL (if applicable)	9. PROCUREMENT INSTRUMENT IDENTIFICATION NUMBER AFOSR-83-0373	
8c. ADDRESS (City, State, and ZIP Code) Building 410, Bolling AFB DC 20332-6448		10. SOURCE OF FUNDING NUMBERS	
		PROGRAM ELEMENT NO. 61102F	PROJECT NO. 2308
		TASK NO. A2	WORK UNIT ACCESSION NO.
11. TITLE (Include Security Classification) (U) Basic Instability Mechanisms in Chemically Reacting Subsonic and Supersonic Flows			
12. PERSONAL AUTHOR(S) Tau-Yi Toong			
13a. TYPE OF REPORT Annual Technical Report	13b. TIME COVERED FROM 30/9/86 TO 29/9/87	14. DATE OF REPORT (Year, Month, Day) 1987, October, 23	15. PAGE COUNT 30
16. SUPPLEMENTARY NOTATION			
17. COSATI CODES	FIELD 21	GROUP 01	18. SUBJECT TERMS (Continue on reverse if necessary and identify by block number) Turbulence-Combustion Interactions Instability Mechanisms Disturbed and Turbulent Flames
20. DISTRIBUTION/AVAILABILITY OF ABSTRACT <input checked="" type="checkbox"/> UNCLASSIFIED/UNLIMITED <input checked="" type="checkbox"/> SAME AS RPT <input type="checkbox"/> DTIC USERS	21. ABSTRACT SECURITY CLASSIFICATION Unclassified		
22a. NAME OF RESPONSIBLE INDIVIDUAL Julian M Tishkoff	22b. TELEPHONE (Include Area Code) (202) 767-4935	22c. OFFICE SYMBOL AFOSR/NA	

19.

and experiments was given at the Yale University.



Accession For	
NTIS GRAZI	<input checked="" type="checkbox"/>
DJIC TAB	<input type="checkbox"/>
Unbalanced	<input type="checkbox"/>
Identification	<input type="checkbox"/>
By _____	
Classification/	
Available Copy Right	
Avail. and/or	
Ref. Special	

A vertical file number 'A-1' is handwritten next to the form.

AFOSR TR. ^ 7 - 1889

ANNUAL TECHNICAL REPORT ON RESEARCH
SUPPORTED BY GRANT AFOSR-83-0373
(September 30, 1986-September 29, 1987)

Basic Instability Mechanisms
in Chemically Reacting Subsonic and Supersonic Flows
Tau-Yi Toong
Massachusetts Institute of Technology

Summary of Progress

The nature of turbulence-combustion interactions was examined by the use of simultaneous dual-thermocouple and LDV-thermocouple measurements, which showed that the presence of the high-frequency velocity (in a direction normal to the flame brush) and temperature fluctuations within slowly drifting turbulent premixed V-flames was associated with changes in the flame shapes, thicknesses, and propagation speeds. Unlike the RMS normal-velocity fluctuations which assumed maximum values within the reaction zone, the RMS tangential-velocity fluctuations remained almost constant, implying that the flame-generated turbulence was in the normal direction. Furthermore, cross-correlation coefficients of simultaneous velocity and temperature fluctuations remained positive within the flame, with values involving normal velocities higher than those involving tangential components.

A paper on the thermal structure of turbulent flames was presented at the Fall Technical Meeting of the Eastern Section of the Combustion

Institute. Another paper on the thermal structure at low Damköhler's numbers was submitted for publication in the Combustion Science and Technology. A seminar on the evolution of turbulence-combustion interactions — theory and experiments was given at the Yale University.

I. Objectives and Scope of Work

The main objectives of this research are to determine and elucidate major mechanisms governing turbulence-combustion interactions in different spectral regimes and to provide sound basis for formulating guidelines for improving combustion efficiency and reducing emissions. During the past year, the nature of these interactions was examined by the use of simultaneous dual-thermocouple and LDV-thermocouple measurements, which showed that the presence of the high-frequency velocity (in a direction normal to the flame brush) and temperature fluctuations within slowly drifting turbulent premixed V-flames was associated with changes in the flame shapes, thicknesses, and propagation speeds. Cross-correlation coefficients of these simultaneous signals assumed rather high values within the reaction zone. However, correlation coefficients of simultaneous temperature and velocity fluctuations in the tangential direction were lower. Unlike the RMS normal-velocity fluctuations which assumed maximum values within the reaction zone, the RMS tangential-velocity fluctuations remained almost the same across the flame, implying that any flame-generated turbulence due to turbulence-combustion interactions was in the normal direction.

A paper on the thermal structure of turbulent flames was presented at the Fall Technical Meeting of the Eastern Section of the Combustion Institute. Another paper on the thermal structure at low Damköhler's numbers was submitted for publication in the Combustion Science and Technology. A seminar on the evolution of turbulence-combustion interactions — theory and experiments was given at the Yale University.

II. Results and Discussions

In order to shed light on the nature of the turbulence-combustion interactions, experiments were conducted to examine the relationships between simultaneous instantaneous temperatures and velocities (either normal or tangential to the flame brush) within the turbulent flame. This study showed that the high-frequency fluctuations in temperatures and normal velocities were highly correlated and were associated with changes in flame shapes, thicknesses, and propagation speeds. Furthermore, their RMS values were higher within the reaction zone than in either the cold or hot regions. However, the fluctuations in tangential velocities were less well correlated with temperatures and their RMS values remained almost constant within the flame brush.

The evolution of turbulence-combustion interactions was examined in three types of simultaneous measurements:

- (1) dual-thermocouple measurements at different distances apart
- (2) normal velocity-temperature measurements
- (3) dual-thermocouple in conjunction with normal or tangential velocity measurements.

They are described in the following sections.

(1) Simultaneous Dual-Thermocouple Measurements

Instantaneous temperatures within turbulent, premixed, lean, chemically pure methane/air, unconfined V-flames stabilized behind a 2.1 mm-diameter cylindrical flameholder were monitored simultaneously by the use of two fine-wire, frequency-compensated thermocouples at

different distances apart. "Instantaneous" mean temperature profile of the slowly drifting flame was determined by analyzing the variation of the corresponding mean temperatures at the two positions. The instantaneous temperature profiles, however, assumed different shapes and thicknesses in the presence of the higher-frequency fluctuations. The instantaneous temperatures rose in the region where the average temperature gradient between the two positions was higher than the value corresponding to the "instantaneous" mean temperature profile (or where the flame was relatively thinner) and dropped in the region where the average gradient was lower, thus leading to the observed higher-frequency temperature fluctuations. Furthermore, the rates of the temperature rise and drop assumed maximum values at the instants when the temperature gradient was the largest (or the turbulent flame was the thinnest) and the smallest (or the flame was the thickest), respectively. Since the temperature gradient and the flame thickness were in some respects related to the turbulence intensity, the temperature rise and drop which resulted in the high-frequency fluctuations were presumably due to varying degrees of turbulence-combustion interactions.

Examination of the spatial cross-correlations of the simultaneous temperatures at different distances apart showed that the integral scale of the eddies responsible for the high-frequency fluctuations was less than 1 mm and that for the low-frequency drifting was larger. (For comparison, note that the corresponding laminar-flame thickness reported in the literature was about 1.5 mm.) These results seemed to be consistent

with Damköhler's conceptual model* that rate-augmentation within turbulent flames was due to eddies smaller in size than the laminar-flame thickness.

(a) Most Probable Instantaneous Temperature Profile

Examination of the simultaneous instantaneous temperatures monitored by two thermocouples 0.3 mm apart in a direction normal to the burner axis showed that they were essentially in phase within a major part of the turbulent flame. Figure 1a shows a segment of the simultaneous temperature signals, together with the corresponding "instantaneous" mean temperatures computed within 25-ms time intervals. Also shown is the difference of the corresponding T_1 (at a position closer to the hot products) and T_2 . Since the two positions were at a fixed distance apart (0.3 mm), this temperature difference also represented the instantaneous, average, local temperature gradient within the turbulent flame. Note that the rates of the rise and of the drop in T_1 and T_2 were roughly the maximum at the instants when the temperature-gradient curve was at its peak and valley, respectively.

Figure 1b shows the variation of T_2 with T_1 at the instants designated. (As shown in Figure 1a, each unit of 5 corresponded to 1 ms intervals.) Also shown are reference lines indicating constant temperature difference between T_1 and T_2 . The counter-clockwise trajectories indicated by the arrows showed that both T_1 and T_2 rose in the region of larger temperature difference or larger average temperature gradient and dropped in the region of smaller temperature gradient. The sizes of the loops described

*Damköhler, G. (1940). Der Einfluss der Turbulenz auf die Flammengeschwindigkeit in Gasgemischen. Z. Elektrochem. Angew. Phys. Chem. 46, 601; (1947). Engl. trans.: The effect of turbulence on the flame velocity in gas mixtures. NACA Tech. Mem. 1112.

by the trajectories were related to the amplitudes of the high-frequency fluctuations in both the temperatures and temperature gradients.

Examination of the corresponding values of T_1 and T_2 over time intervals longer than the characteristic time for low-frequency drifting (of about 200 ms) showed that the data scattered about a most probable curve represented by curve S_1 in Figure 2a. Curves S_2 and S_3 denoted the boundaries of data scatter one standard deviation away, with S_2 traversing in the region of larger temperature gradients (cf. the reference constant temperature-difference curves) and S_3 in the region of smaller temperature gradients. The most probable instantaneous temperature profile derived from curve S_1 is shown in Figure 2b. The instantaneous temperature profiles corresponding to the boundaries of data scatter one standard deviation away are also shown in Figure 2b. On the basis of the maximum slopes through the inflection points of the temperature profiles, the most probable instantaneous flame thickness was about 1.5 mm. Due to the presence of the high-frequency fluctuations, the profiles assumed different shapes, with their thicknesses varying from 1.1 to 2.4 mm, one standard deviation away.

(b) "Instantaneous" Mean Temperature Profile

The "instantaneous" mean temperature profile of the slowly drifting flame was determined by analyzing the variation of the corresponding mean temperatures at the two positions 0.3 mm apart. Figure 3a shows a segment of the simultaneous "instantaneous" mean temperatures \bar{T}_1 and \bar{T}_2 , computed within 25-ms time intervals. Again, they were essentially in phase. Also shown is the difference of the corresponding $(\bar{T}_1 - \bar{T}_2)$, which represented

also the average mean temperature gradient between the two positions. Unlike the instantaneous ($T_1 - T_2$) which fluctuated at high frequencies with moderate amplitudes, as shown in Figure 1a, ($\bar{T}_1 - \bar{T}_2$) here remained almost constant, suggesting little change in the mean temperature gradient as the turbulent flame drifted slowly past the thermocouple locations. Assuming a linear temperature profile for the portion of the flame monitored by the thermocouples, one estimated from Figure 3a that the flame drifted about 0.3 mm in about 50 ms at an average speed of only 6 mm/s.

Figure 3b shows the variation of \bar{T}_2 with \bar{T}_1 over the time interval represented in Figure 3a. Unlike T_2 versus T_1 as shown in Figure 1b, no clear pattern could be discerned in the trajectories, suggesting little change in the shape of the "instantaneous" mean temperature profile of the drifting flame.

Figure 4a shows the most probable variation of \bar{T}_2 versus \bar{T}_1 as represented by curve \bar{S}_1 . Also shown are curves \bar{S}_2 and \bar{S}_3 , which denote the boundaries of data scatter one standard deviation away. Note that the difference between the three curves in Figure 4a is smaller than that in Figure 2a, which shows much larger change in the flame shape due to the presence of the high-frequency fluctuations.

Figure 4b shows the most probable mean temperature profile \bar{S}_1 , together with profiles one standard deviation away. The corresponding flame thicknesses were 1.2, 1.1 and 1.4 mm, respectively, showing that the instantaneous turbulent flame was thicker due to the presence of the high-frequency fluctuations (cf. Figure 2b for comparison between

profiles obtained on the basis of S_1 and \bar{S}_1).

(c) Normalized Spatial Cross-Correlation Coefficients

In order to determine the sizes of the eddies responsible for the high- and the low-frequency fluctuations, the spatial cross-correlations of the simultaneous temperatures at different distances apart within the turbulent flame were obtained. Figure 5a shows the normalized coefficients for the high-frequency fluctuations at 0.3 mm apart at different parts of the drifting flame designated by the corresponding "instantaneous" mean temperatures. Their values were about 0.9 over the major part of the flame, indicating rather high degree of correlation at 0.3 mm separation.

Figure 5b shows the normalized spatial cross-correlation coefficients at different separation distances. For the high-frequency fluctuations, two curves were obtained by the use of different configurations for the support of the thermocouples. (Experiments are still in progress to determine the correlations at larger separation distances.) On the basis of the results obtained so far, one estimated that the integral scale of the relevant eddies here was less than 1 mm. For comparison, one noted that the corresponding laminar-flame thickness at an equivalence ratio of 0.75 was reported in the literature to be 1.5 mm. Thus, the eddies responsible for the high-frequency fluctuations seemed to be smaller in size than the laminar-flame thickness — a conclusion consistent with Damköhler conceptual model.*

Figure 5b also shows the correlation coefficients for the low-frequency

* Cf. footnote on p. 6.

fluctuations. They were higher than those for the high-frequency fluctuations, suggesting that the relevant eddy size was larger.

(2) Simultaneous Normal Velocity-Temperature Measurements

In order to understand the mechanisms governing turbulence-combustion interactions, simultaneous instantaneous velocities (in a direction normal to the flame brush) and temperatures were measured within the turbulent V-flame.* Some of the results, such as the cross-correlation coefficients, RMS values, spectral density distributions, probability density functions, were reported earlier in an annual report, dated October 22, 1986. More recently, these results were further analyzed to shed light on the evolution of the turbulence-combustion interactions.

Figure 6a shows a segment of the simultaneous normal velocities and temperatures, together with the corresponding "instantaneous" mean values computed within 25-ms time intervals. The variation of the corresponding instantaneous velocities and temperatures was shown in Figure 6b at designated instants of time. (As shown in Figure 6a, each unit of 5 represented 1 ms intervals.) The clockwise trajectories (which resulted from the high-frequency fluctuations) showed that at a given temperature the velocity was higher in a region where the temperature was rising or, according to Figure 1b, in a region where the average temperature gradient was larger than that corresponding to the "instantaneous" mean temperature profile or where the flame was thinner (cf. Figure 2).

*For these experiments, the thermocouple was placed 1 mm downstream of the LDV (Laser-Doppler-Velocimetry) monitoring station at an angle 13° from the vertical direction.

The instantaneous mass flux was related to the ratio of the corresponding velocity and temperature, if one assumed that the density-temperature product remained constant for almost same pressure across the flame brush. Figure 7a shows the simultaneous V/T and T , together with the corresponding "instantaneous" mean values computed within 25-ms time intervals for the same segment of data represented in Figure 6. The variation of the corresponding instantaneous values was shown in the trajectories of Figure 7b. Note that at a given temperature the mass flux was higher in a region where the temperature was rising or where the average temperature gradient was larger than that corresponding to the "instantaneous" mean temperature profile (according to Figure 1b). Noting that the mass flux was related to the turbulent flame-propagation speed, one concluded that the propagation speed was higher in a region where the flame was relatively thinner. Thus, due to turbulence-combustion interactions, the turbulent flame changed its structure and propagation speed.

Figure 8 shows the "instantaneous" mean values of (\bar{V}/T) (related to the corresponding mean mass fluxes) at different parts of the slowly drifting flame. Unlike the instantaneous values shown in Figures 7a and b, the mean values were almost constant within the flame, with very small scatter as shown by the spread of the dashed curves which represented boundaries one standard deviation away.

(3) Simultaneous Dual-Thermocouple/Normal or Tangential Velocity Measurements

In order to further elucidate the evolution of the turbulence-combustion interactions, their effects on the flame structure and propagation speeds,

and their governing mechanisms, experiments were initiated to examine the relationships between instantaneous velocities, in directions normal (V) and tangential (U) to the flame brush, and temperatures at two other neighboring locations. The initial results were obtained with one thermocouple (designated as T_1) 1 mm vertically above the LDV station and another thermocouple (designated as T_2) 0.4 mm apart from T_1 in the horizontal direction away from the hot products. Figure 9 shows the projections of the trajectories $V/T_1/T_2$ onto the respective planes T_2 , $T_1; V, T_2$; and V, T_1 . Similar to Figure 1b, the projection on the (T_2, T_1) plane described a counter-clockwise trajectory, with both T_1 and T_2 rising in a region of larger temperature difference or average gradient and dropping in a region of smaller temperature gradient. Also, like Figure 6b, the projection on the (V, T_2) plane described a clockwise trajectory, with higher velocity in a region where the temperature was rising or where the average temperature gradient was larger and the flame was thinner. On the other hand, the projection on the $(V-T_1)$ plane did not seem to exhibit any definitive pattern.

Figures 10a and b show the distributions of the apparent mean normal (\bar{V}) and tangential (\bar{U}) velocities versus the apparent mean temperatures \bar{T}_1 and \bar{T}_2 , respectively. Also shown are the apparent RMS values in temperature and velocity fluctuations. Despite increasing mean normal velocities across the flame brush with rising temperatures, the mean tangential velocities remained almost constant. The RMS temperature and normal-velocity fluctuations assumed distinct maximum values somewhere within the reaction zone, while the RMS tangential-velocity fluctuations did not vary much within the flame.

Similar behaviors were observed in Figures 11a and b for the "instantaneous" mean values and the high-frequency RMS fluctuations.

Normalized cross-correlation coefficients of the simultaneous velocity and temperature fluctuations within the high-frequency region are shown in Figures 12a and b versus the instantaneous mean temperatures \bar{T}_1 and \bar{T}_2 , respectively. They remained positive within the flame for both the normal- and the tangential-velocity fluctuations, thus indicating the inappropriateness of the gradient model to account for turbulent energy transport. Furthermore, the coefficients involving normal velocity components assumed higher values than those involving tangential components. Coupled with the observations in Figures 10 and 11, one suspects that the nature of the turbulence-combustion interactions in the two directions may be different.

Figures 13a and b show, respectively, comparisons of spectral density distributions of apparent all-pass mean-square normal- and tangential-velocity fluctuations at three different positions within the flame. For the normal velocity component (Figure 13a), the values at the position of maximum RMS fluctuations were significantly higher than those in the hot products and the cold reactants (as designated by the corresponding apparent mean temperatures \bar{T}_1 and \bar{T}_2), thus suggesting the presence of flame-generated turbulence. On the other hand, Figure 13b shows that the distribution for the tangential velocity component remained almost the same across the flame, again implying that the nature of the turbulence-combustion interactions in the tangential direction may be different from that in the normal direction.

III. Publications and Reports

See attached Enclosure.

IV. Professional Personnel

Professor T. Y. Toong.

V. Interactions

A presentation on Thermal Structure of Turbulent Premixed Rod-Stabilized V-Flames was made by T. Y. Toong on December 15, 1986 at the 1986 Fall Technical Meeting, Eastern Section of the Combustion Institute, Hotel Condado Beach, San Juan, Puerto Rico.

A seminar on Evolution of Turbulence-Combustion Interactions — Theory and Experiments was given by T. Y. Toong on April 2, 1987 at the Yale University, New Haven, CT.

A presentation on Evolution of Turbulence-Combustion Interactions was made by T. Y. Toong on June 22, 1987 at the 1987 AFOSR/ONR Contractors Meeting on Propulsion Research, Pennsylvania State University, University Park, PA.

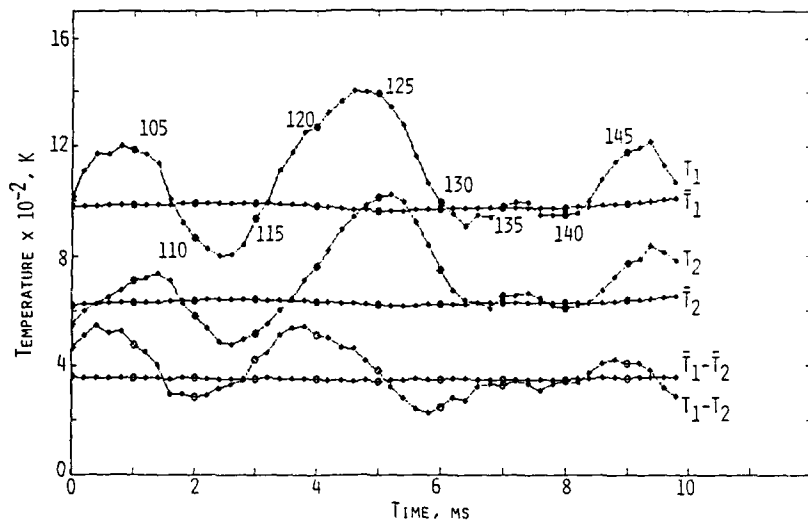


FIG. 1A SIMULTANEOUS INSTANTANEOUS TEMPERATURES 0.3 MM APART AND CORRESPONDING "INSTANTANEOUS" MEAN TEMPERATURES. TURBULENT FLAME WITH 10-MESH GRID, EQUIVALENCE RATIO, 0.75; MEAN MIXTURE VELOCITY, 2.4 M/S; 35 MM DOWNSTREAM OF 2.1 MM-DIAMETER FLAMEHOLDER.

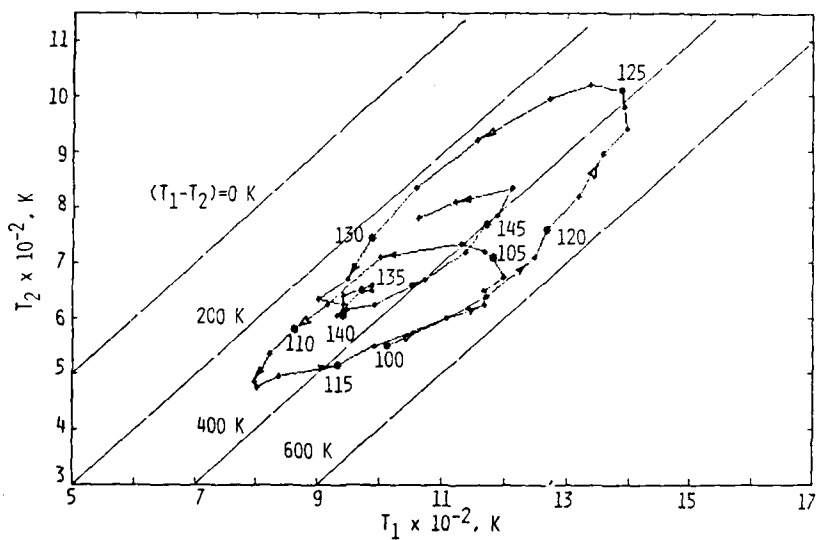


FIG. 1B TRAJECTORIES SHOWING VARIATION OF T_2 WITH T_1 , 0.3 MM APART, AT THE INSTANTS DESIGNATED. DASHED LINES INDICATING CONSTANT TEMPERATURE DIFFERENCE BETWEEN T_1 AND T_2 .

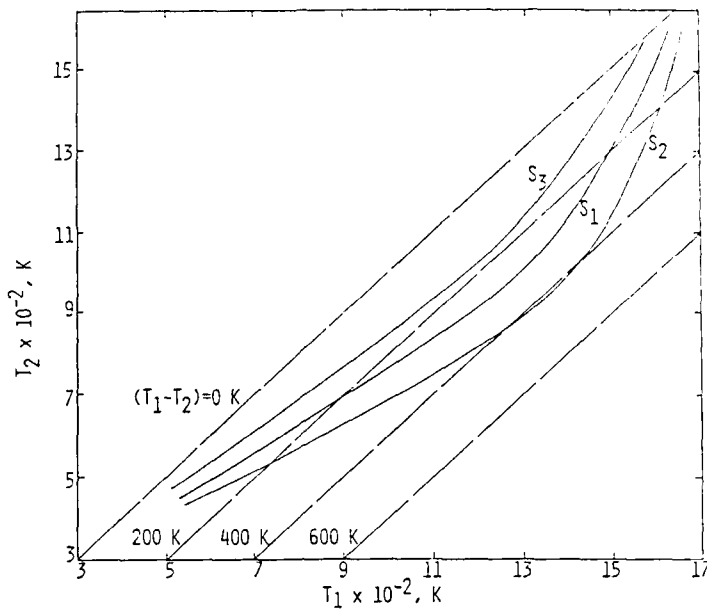


FIG. 2A VARIATION OF T_2 WITH T_1 , 0.3 MM APART. S_1 , MOST PROBABLE DISTRIBUTION; S_2 AND S_3 , ONE STANDARD DEVIATION AWAY. DASHED LINES INDICATING CONSTANT TEMPERATURE DIFFERENCE.

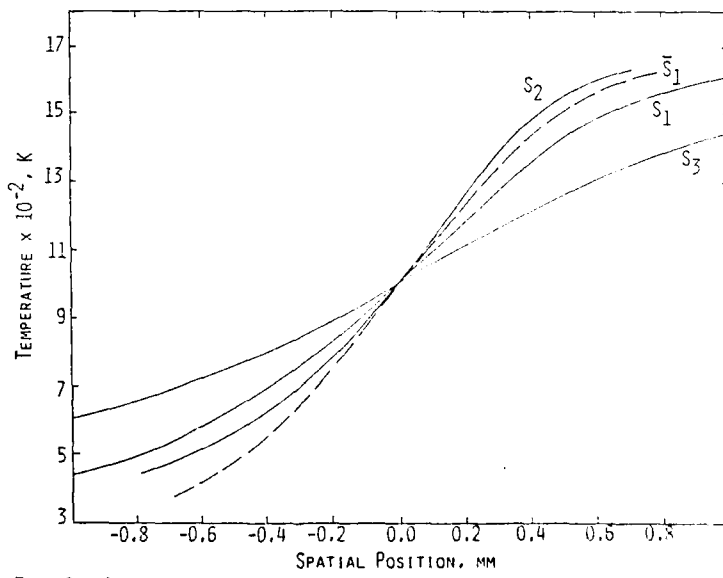


FIG. 2B INSTANTANEOUS TEMPERATURE PROFILES: S_1 , MOST PROBABLE DISTRIBUTION; S_2 AND S_3 , ONE STANDARD DEVIATION AWAY. COMPARISON WITH MOST PROBABLE "INSTANTANEOUS" MEAN TEMPERATURE PROFILE \bar{S}_1 .

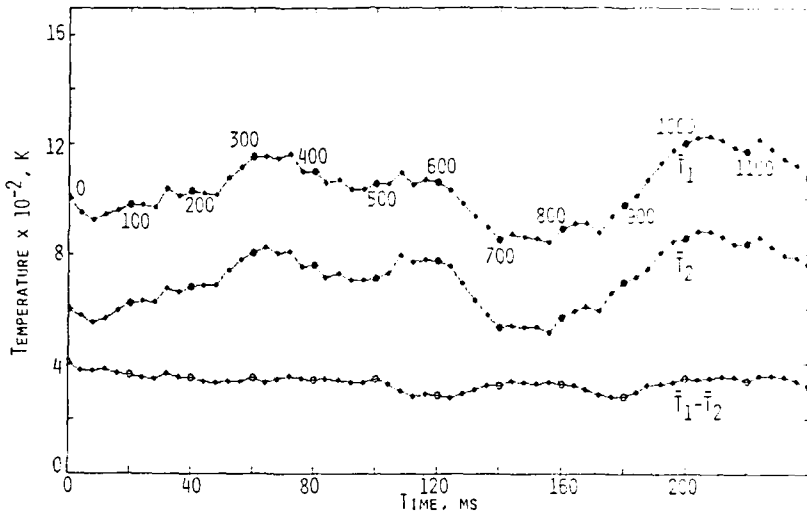


FIG. 3A SIMULTANEOUS "INSTANTANEOUS" MEAN TEMPERATURES, 0.3 MM APART, COMPUTED WITHIN 25-MS TIME INTERVALS. TURBULENT FLAME WITH 10-MESH GRID, EQUIVALENCE RATIO, 0.75; MEAN MIXTURE VELOCITY, 2.4 M/S; 35 MM DOWNSTREAM OF 2.1 MM-DIAMETER FLAMEHOLDER.

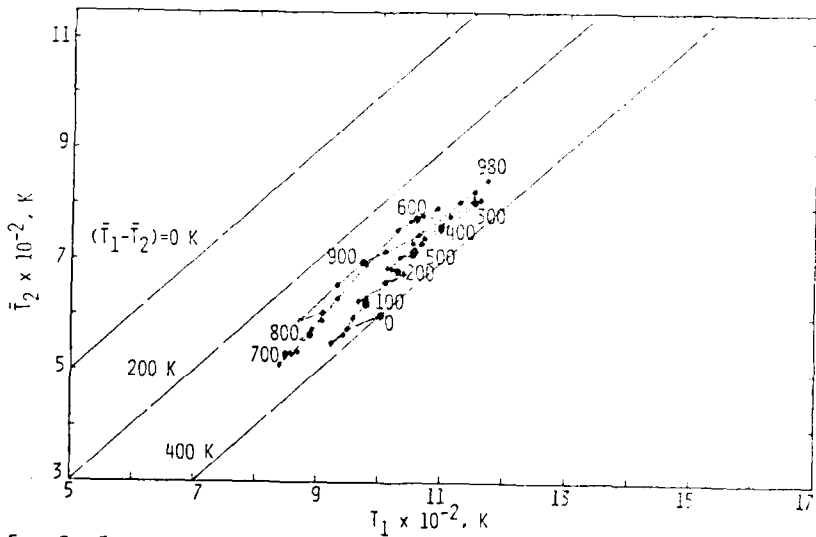


FIG. 3B TRAJECTORIES SHOWING VARIATION OF \bar{T}_2 WITH \bar{T}_1 , 0.3 MM APART. DASHED LINES INDICATING CONSTANT TEMPERATURE DIFFERENCE BETWEEN \bar{T}_1 AND \bar{T}_2 .

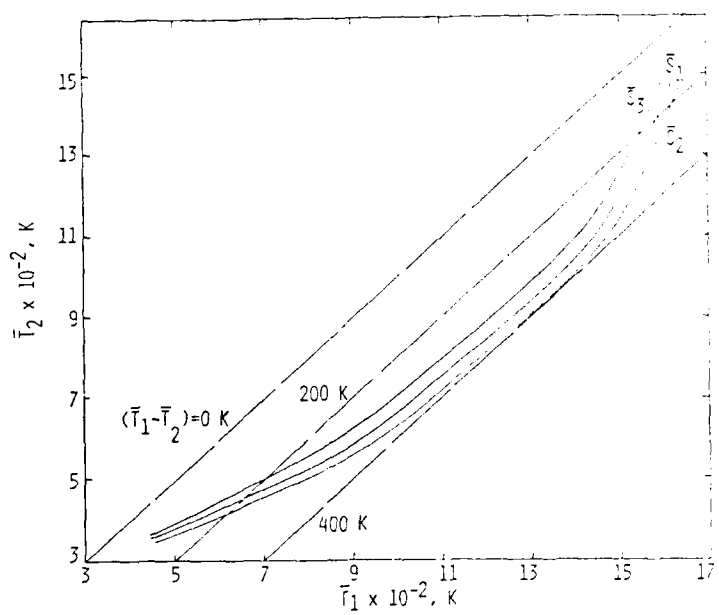


FIG. 4A VARIATION OF \bar{T}_2 WITH \bar{T}_1 , 0.3 MM APART. \bar{S}_1 , MOST PROBABLE DISTRIBUTION; \bar{S}_2 AND \bar{S}_3 , ONE STANDARD DEVIATION AWAY. DASHED LINES INDICATING CONSTANT TEMPERATURE DIFFERENCE.

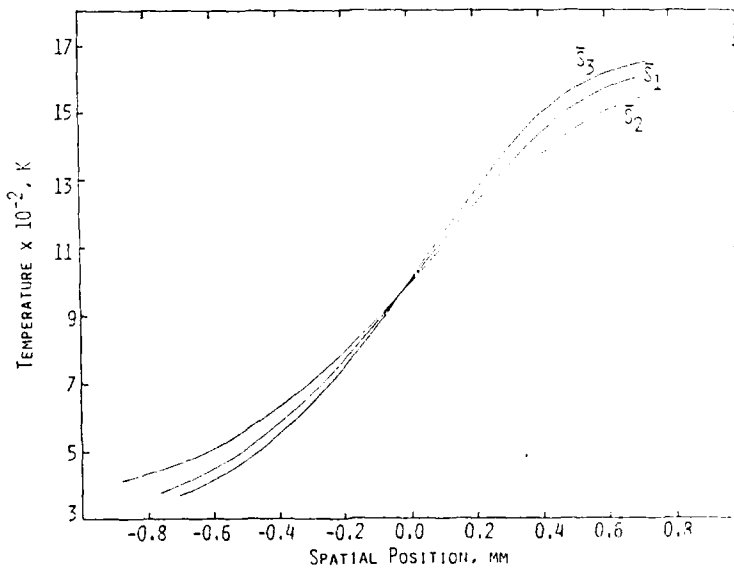


FIG. 4B "INSTANTANEOUS" MEAN TEMPERATURE PROFILES. \bar{S}_1 , MOST PROBABLE DISTRIBUTION; \bar{S}_2 AND \bar{S}_3 , ONE STANDARD DEVIATION AWAY.

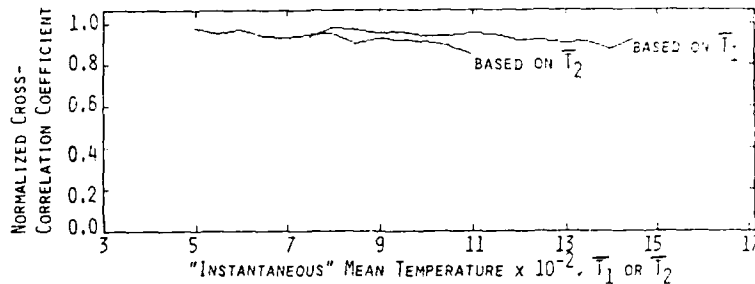


FIG. 5A NORMALIZED CROSS-CORRELATION COEFFICIENTS FOR THE HIGH-FREQUENCY FLUCTUATIONS, 0.3 MM APART, AT DIFFERENT PARTS OF THE SLOWLY DRIFTING TURBULENT FLAME. 10-MESH GRID; EQUIVALENCE RATIO, 0.75; MEAN MIXTURE VELOCITY 2.4 M/S; 35 MM DOWNSTREAM OF 2.1 MM-DIAMETER FLAMEHOLDER.

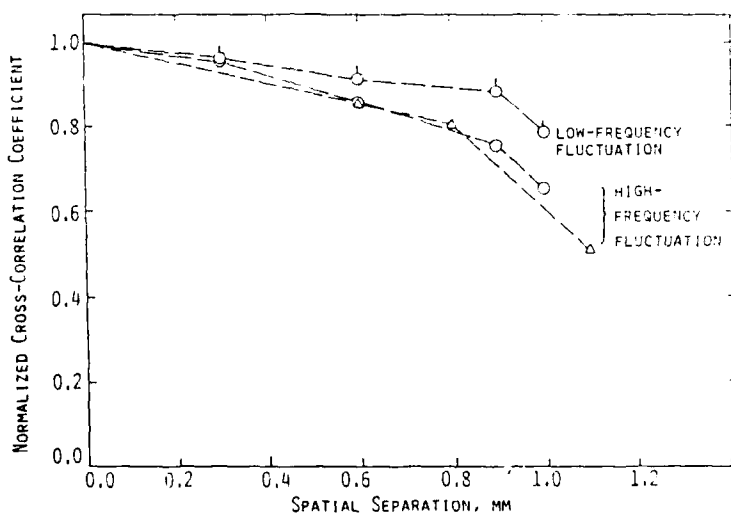


FIG. 5B NORMALIZED CROSS-CORRELATION COEFFICIENTS AT DIFFERENT SPATIAL SEPARATION DISTANCES. \circ , Δ , HIGH-FREQUENCY FLUCTUATIONS;
 \circ , LOW-FREQUENCY FLUCTUATIONS.

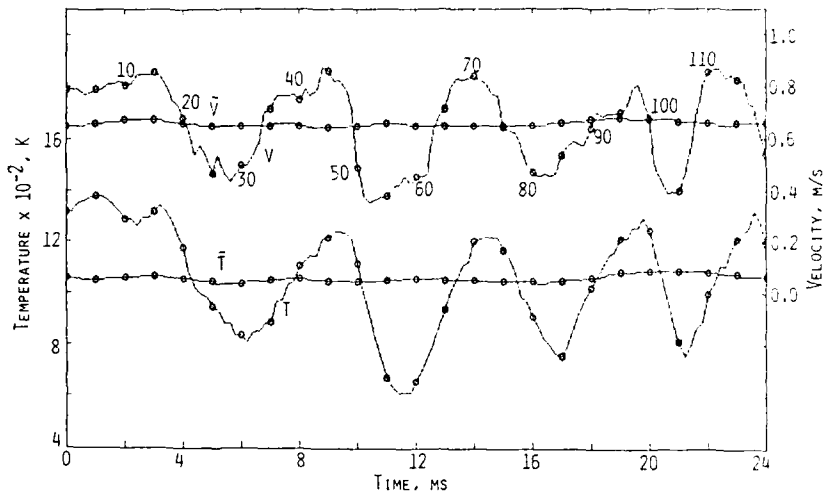


FIG. 6A SIMULTANEOUS INSTANTANEOUS NORMAL VELOCITIES AND TEMPERATURES, 1 MM APART, AND CORRESPONDING "INSTANTANEOUS" MEAN VALUES. TURBULENT FLAME WITH 10-MESH GRID, EQUIVALENCE RATIO, 0.75; MEAN MIXTURE VELOCITY, 2.4 M/S; 35 MM DOWNSTREAM OF 2.1 MM-DIAMETER FLAMEHOLDER.

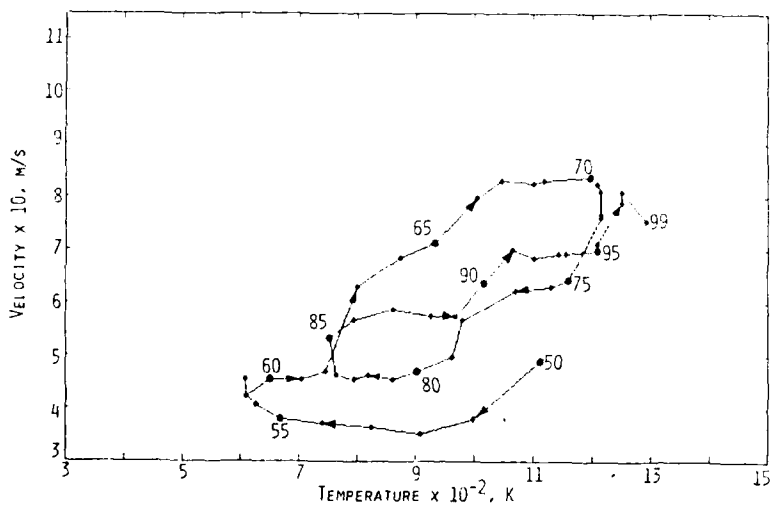


FIG. 6B TRAJECTORIES SHOWING VARIATION OF NORMAL VELOCITY WITH TEMPERATURE, 1 MM APART, AT THE INSTANTS DESIGNATED.

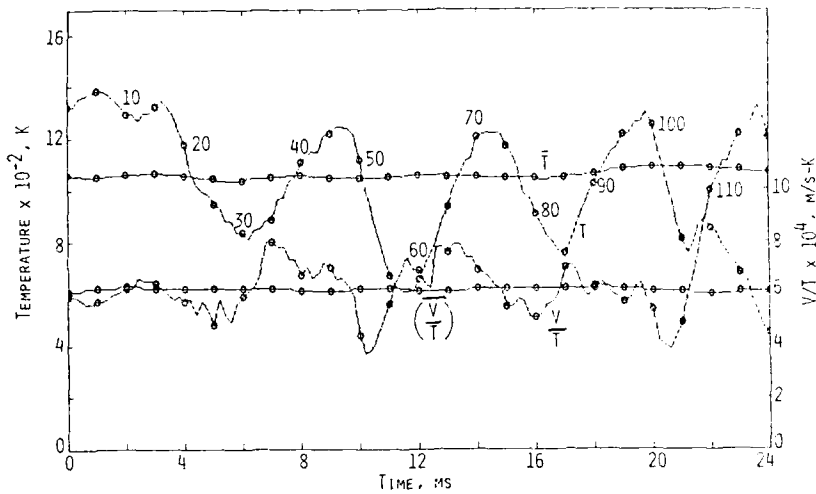


FIG. 7A SIMULTANEOUS INSTANTANEOUS TEMPERATURES AND NORMAL-VELOCITY/TEMPERATURE RATIOS, 1 MM APART, AND CORRESPONDING "INSTANTANEOUS" MEAN VALUES.

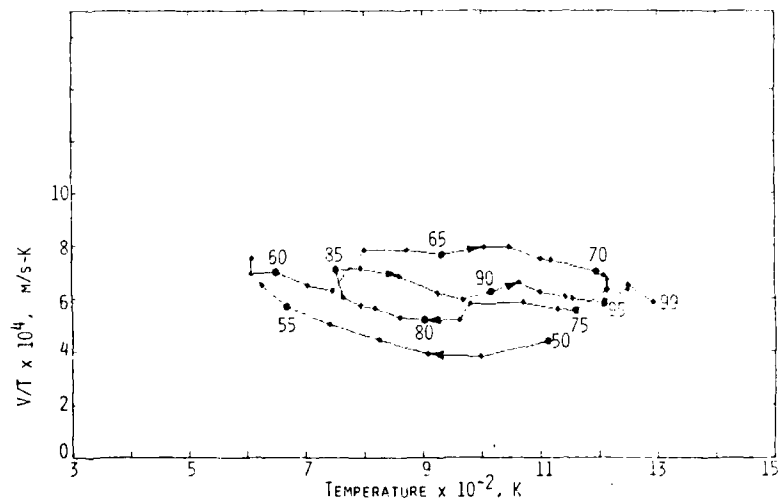


FIG. 7B TRAJECTORIES SHOWING VARIATION OF NORMAL-VELOCITY/TEMPERATURE RATIO WITH TEMPERATURE, 1 MM APART, AT THE INSTANTS DESIGNATED.

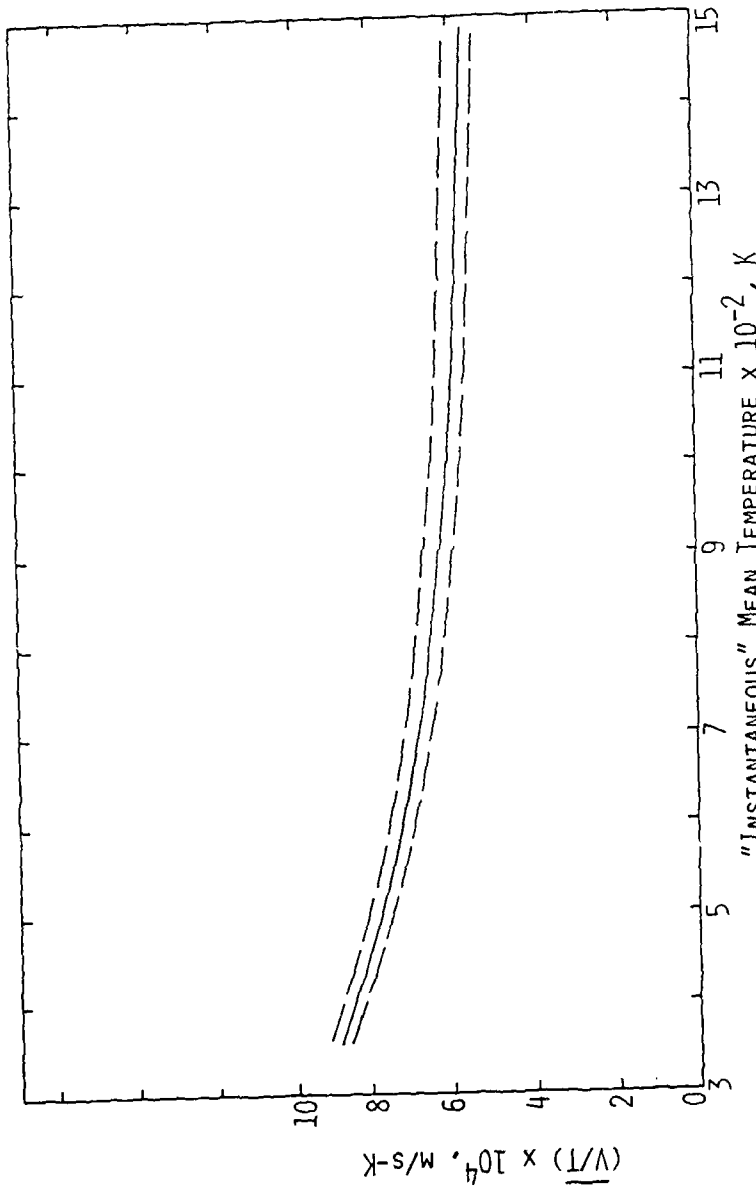


FIG. 8 "INSTANTANEOUS" MEAN TEMPERATURE $\times 10^{-2}$, K
"INSTANTANEOUS" MEAN VALUES OF (V/\bar{T}) AT DIFFERENT PARTS OF THE SLOWLY
DRIFTING TURBULENT FLAME. DASHED LINES SHOWING BOUNDARIES OF SCATTER ONE
STANDARD DEVIATION AWAY.

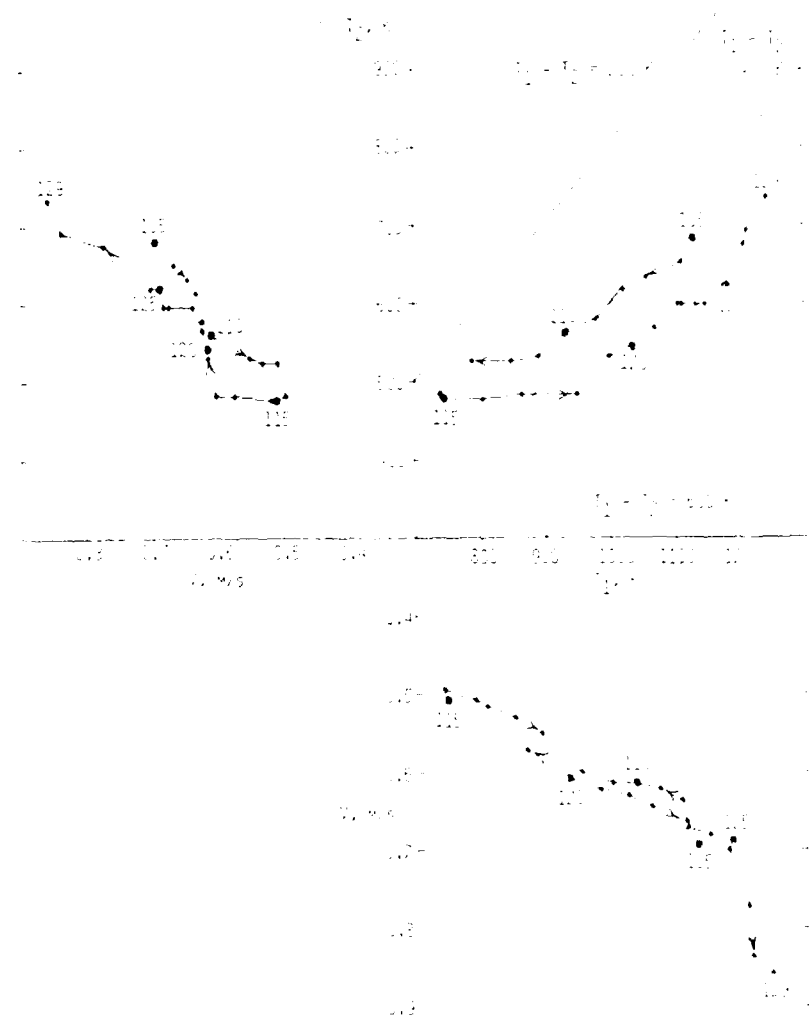


FIG. 3 PROJECTIONS OF NORMAL VELOCITY/TEMPERATURE/TEMPERATURE TRAJECTORIES SHOWING VARIATION OF V WITH T_2 , V WITH $T_1 - T_2$ AND V WITH T_1 AT THE INSTANTS DESIGNATED. (DASHED LINES INDICATING CONSTANT TEMPERATURE DIFFERENCE BETWEEN T_1 AND T_2).

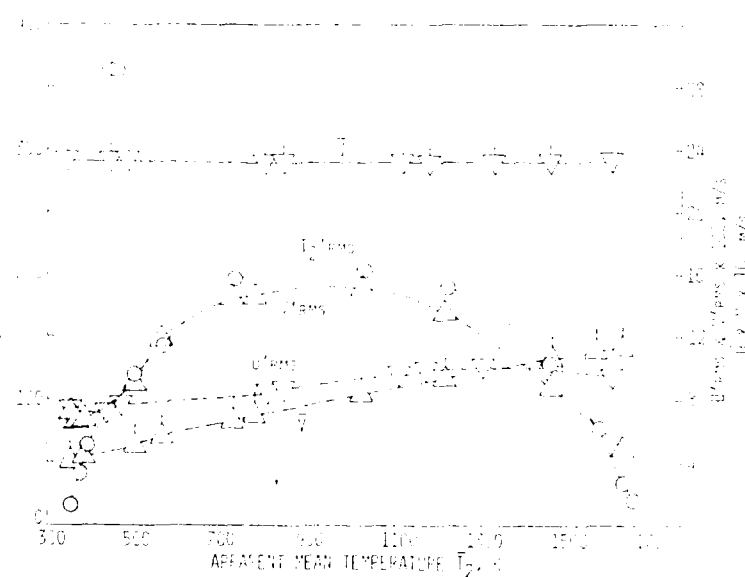
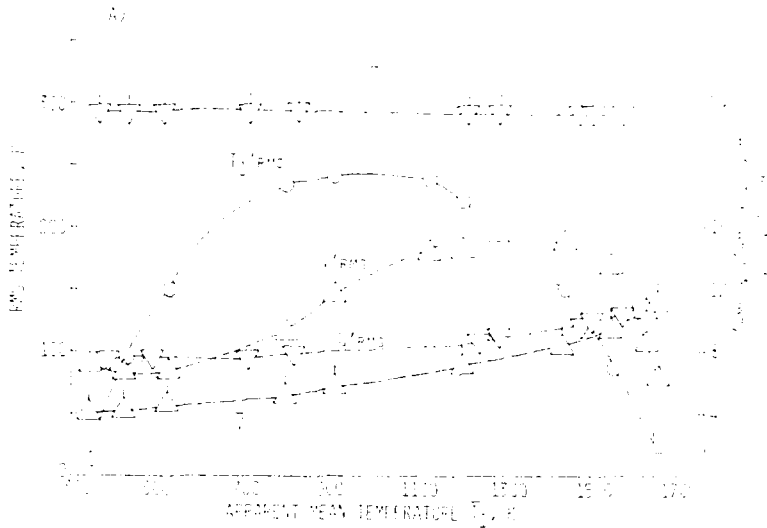


FIG. 10 APPARENT MEAN NORMAL VELOCITY (\bar{U}_n), MEAN TANGENTIAL VELOCITY (\bar{U}_t), AND TEMPERATURE (\bar{T}_1 , \bar{T}_2) AND VELOCITY (U_1' , U_2') FLUCTUATION VERSUS APPARENT MEAN TEMPERATURES (\bar{T}_1 , \bar{T}_2).

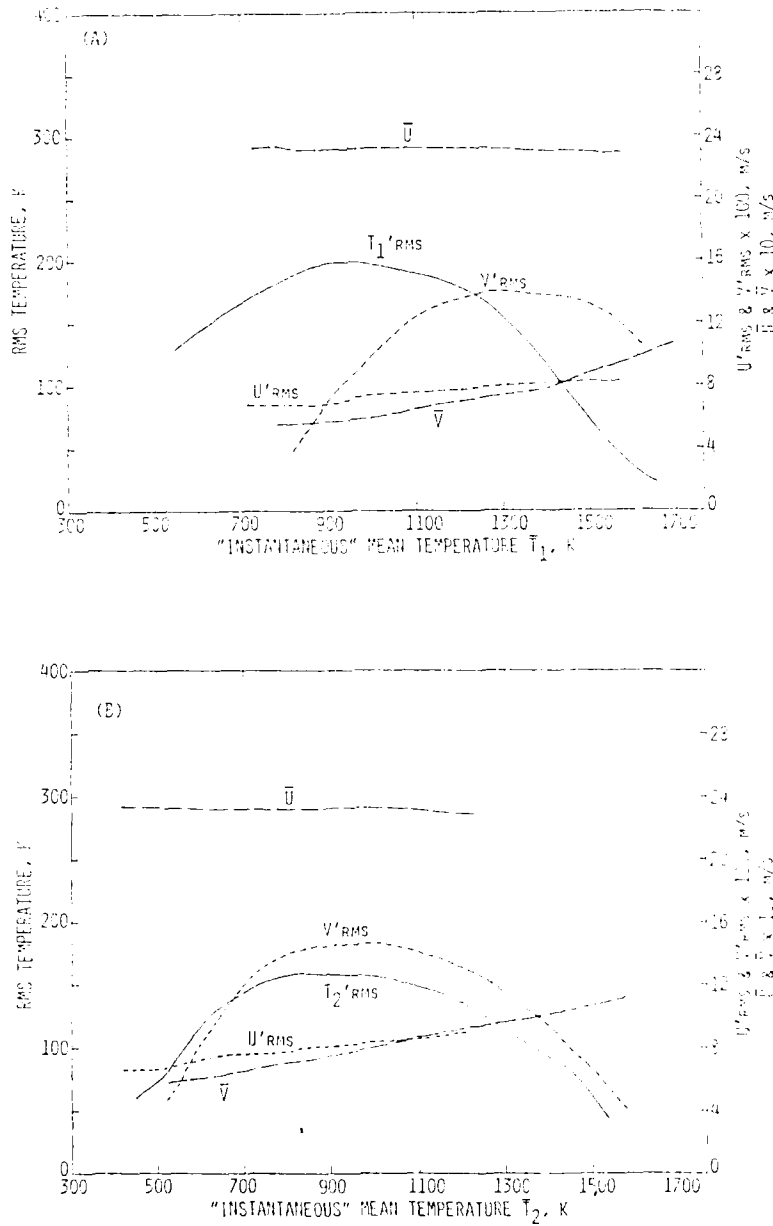


FIG. 11 COMPARISON OF MEAN NORMAL VELOCITY (\bar{V}), MEAN TANGENTIAL VELOCITY (\bar{U}), AND RMS TEMPERATURE (T_1' , T_2') AND VELOCITY (U' , V') FLUCTUATIONS WITHIN HIGH-FREQUENCY REGION AT DIFFERENT "INSTANTANEOUS" MEAN TEMPERATURES (\bar{T}_1 , \bar{T}_2).

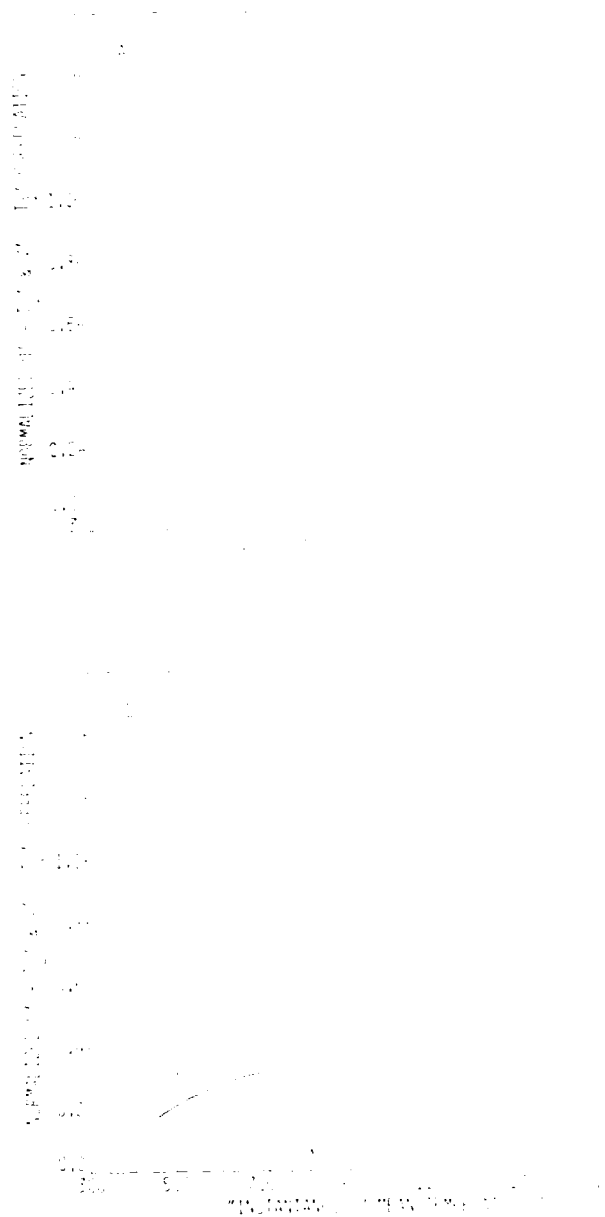


FIG. 12 COMPARISON OF NORMALIZED THERMAL RESISTANCE COEFFICIENTS WITHIN VARIOUS MATERIALS AS A FUNCTION OF "INSTANTANEOUS" MEAN TEMPERATURE

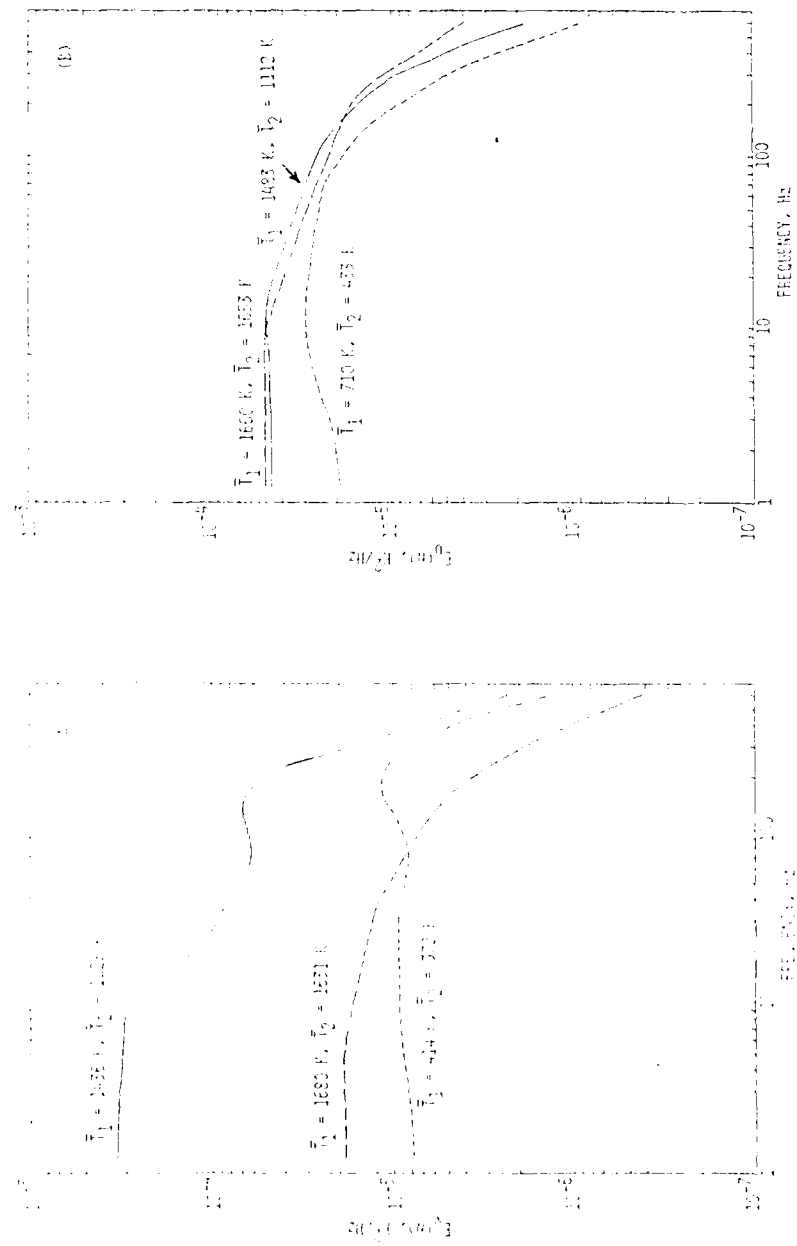


Fig. 13 COMPARISON OF SPECTRAL DENSITY DISTRIBUTIONS OF APPARENT ALL-PASS MEAN-SQUARE NORMAL (A) AND TANGENTIAL (E) VELOCITY FLUCTUATIONS AT THREE DIFFERENT POSITIONS DESIGNATED BY CORRESPONDING APPARENT MEAN TEMPERATURES (\bar{T}_1 , \bar{T}_2),

ENCLOSURE

Basic Instability Mechanisms
in Chemically Reacting Subsonic and Supersonic Flows
Publications and Reports
(Grant AFOSR-83-0373)

1. Abouseif, G. E., Keklak, J. A. and Toong, T. Y., "Ramjet Rumble: The Low-Frequency Instability Mechanism in Coaxial Dump Combustors", Combustion Science and Technology, 36, pp. 83-108, 1984.
2. Abouseif, G. E. and Toong, T. Y., "Theory of Unstable Two-Dimensional Detonations: Genesis of Transverse Waves", Combustion and Flame, 63, pp. 191-207, 1986.
3. Toong, T. Y. and Chang, C., "Thermal Structure of Turbulent Premixed Rod-Stabilized V-Flames", the Fall Technical Meeting, Eastern Section, Combustion Institute, 1986.
4. Toong, T. Y. and Chang, C., "Thermal Structure of Turbulent Premixed Rod-Stabilized V-Flames at Low Damköhler's Numbers", submitted for publication in the Combustion Science and Technology, 1987.

END

DATE

- FILMED

4 88

OPTION